The *cis* acting sequences responsible for the differential decay of the unstable MFA2 and stable PGK1 transcripts in yeast include the context of the translational start codon

THOMAS LaGRANDEUR and ROY PARKER

Department of Molecular and Cellular Biology & Howard Hughes Medical Institute,
University of Arizona, Tucson, Arizona 85721, USA

ABSTRACT

A general pathway of mRNA turnover has been described for yeast in which the 3′ poly(A) tail is first deadenylated to an oligo(A) length, leading to decapping and subsequent 5′–3′ exonucleolytic decay. The unstable MFA2 mRNA and the stable PGK1 mRNAs both decay through this pathway, albeit at different rates of deadenylation and decapping. To determine the regions of the mRNAs that are responsible for these differences, we examined the decay of chimeric mRNAs derived from the 5′ untranslated, coding, and 3′ untranslated regions of these two mRNAs. These experiments have led to the identification of the features of these mRNAs that lead to their different stabilities. The MFA2 mRNA is unstable solely because its 3′ UTR promotes the rates of deadenylation and decapping; all other features of this mRNA are neutral with respect to mRNA decay rates. The PGK1 mRNA is stable because the sequence context of the PGK1 translation start codon and the coding region function together to stabilize the transcript, whereas the PGK1 3′ UTR is neutral with respect to decay. Importantly, changes in the PGK1 start codon context that destabilized the transcript also reduced its translational efficiency. This observation suggests that the nature of the translation initiation complex modulates the rates of mRNA decapping and decay.

Keywords: decay; mRNA; turnover; yeast

INTRODUCTION

The degradation of mRNA is a key aspect of gene expression because mRNA decay rates vary substantially, and can be modulated in response to specific physiological cues. The differential degradation of transcripts has focused attention on the molecular mechanisms that allow specific transcripts to be degraded at distinct rates. Insight into the control of mRNA degradation rates has come from the identification of the pathways for mRNA turnover, and the critical steps in those pathways that affect the rates of mRNA degradation (for review, see Beelman & Parker, 1995; Ross, 1995; Caponigro & Parker, 1996; Jacobson & Peltz, 1996). These pathways include endonucleolytic cleavage (Nielsen & Christiansen, 1992; Brown et al., 1993; Presutti et al., 1995), decapping followed by 5′-to-3′ exonucleolytic degradation (Muhlrad & Parker, 1994;

Gera & Baker, 1998), and degradation induced by deadenylation, which can lead either to decapping and 5′-to-3′ degradation (Muhlrad & Parker, 1992; Decker & Parker, 1993; Hsu & Stevens, 1993; Muhlrad et al., 1994, 1995), or 3′-to-5′ exonucleolytic digestion (Jacobs Anderson & Parker, 1998). Based on experiments in the yeast *Saccharomyces cerevisiae*, the major pathway of mRNA decay occurs by a deadenylation dependent decapping reaction, thereby exposing the transcript to rapid 5′-to-3′ exonucleolytic degradation (Decker & Parker, 1993; Hsu & Stevens, 1993; Muhlrad et al., 1994, 1995).

The decay rate of a given yeast mRNA through the deadenylation-dependent decapping pathway can be attributed to differences in the rates of both deadenylation and decapping. Given this fact, the determination of the basis for differences in rates of deadenylation and decapping will be important for understanding mRNA turnover. Based on the observations that specific mRNA sequences can affect mRNA decay rates (for review, see Ross, 1995; Caponigro & Parker, 1996; Jacobson & Peltz, 1996), a general model for the con-

trol of mRNA turnover can be proposed. In this model, the activities of the decay machinery would be modulated from basal rates by specific sequence elements within a given mRNA. Such "instability" or "stability" sequences presumably would be recognized by *trans*-acting gene products that mediate the rates of decay, by ultimately affecting either deadenylation and/or decapping rates.

To understand how specific sequences within yeast transcripts determine rates of decay through the deadenylation-dependent decapping pathway, an important step will be to define the sequences that modulate deadenylation and decapping rates. To address this issue, we chose to identify the regions of the MFA2 and PGK1 mRNAs that are responsible for their relative rates of decay. These mRNAs were ideal to compare in this analysis for several reasons. First, they represent the extremes of mRNA stability in yeast, as the MFA2 mRNA is unstable ($t_{1/2}$ = 4 min) and the PGK1 transcript is stable ($t_{1/2}$ = 45 min; Herrick et al., 1990). Second, the decay of these mRNAs has been well characterized, indicating that they are both degraded by the same pathway of turnover (Muhlrad et al., 1994, 1995). For instance, the decay of these mRNAs is dependent on the same decapping enzyme and 5'-to-3' exonuclease (Muhlrad et al., 1994, 1995; Beelman et al., 1996). Finally, the different rates of mRNA degradation of these two transcripts can be attributed to specific steps in mRNA turnover. The unstable MFA2 transcript deadenylates more rapidly (~13 As/min) than does the stable PGK1 transcript (~4 As/min; Decker & Parker, 1993). Similarly, the MFA2 transcript is decapped rapidly, whereas the PGK1 transcript is decapped slowly (Muhlrad et al., 1994, 1995). Thus, we postulate that specific features of these mRNAs dictate different rates of cleavage by the same enzymes. Indeed, previous experiments had demonstrated that the MFA2 3' untranslated region (UTR) contained sequences that could promote mRNA degradation (Muhlrad & Parker, 1992), although the role of the 5' UTR and the coding region in mRNA decay had not been examined.

To more fully determine the features of the MFA2 and PGK1 mRNAs that contribute to their respective stabilities, we took a systematic approach of constructing and analyzing chimeric transcripts derived from the two mRNAs. Specifically, we constructed chimeric mRNAs from the 5' UTR, coding region, and 3' UTR of these mRNAs, and then measured the decay rates of these transcripts. The basis for differences in rates of decay was also examined as a function of relative rates of deadenylation and decapping. In agreement with previous results, the instability of the MFA2 mRNA was specified by its 3' UTR (Muhlrad & Parker, 1992). Surprisingly, the stability of the PGK1 mRNA was dependent on both the sequence context of the PGK1 translation start codon and the PGK1 coding region. Alteration of the context of the PGK1 start codon re-

duced both the stability and the translational efficiency of the transcript. The start codon context and coding regions therefore appear to stabilize the PGK1 mRNA by promoting efficient translation of the transcript in a manner that inhibits mRNA turnover. This observation is consistent with the hypothesis that the nature of the translation initiation complex modulates the rates of mRNA decapping and decay.
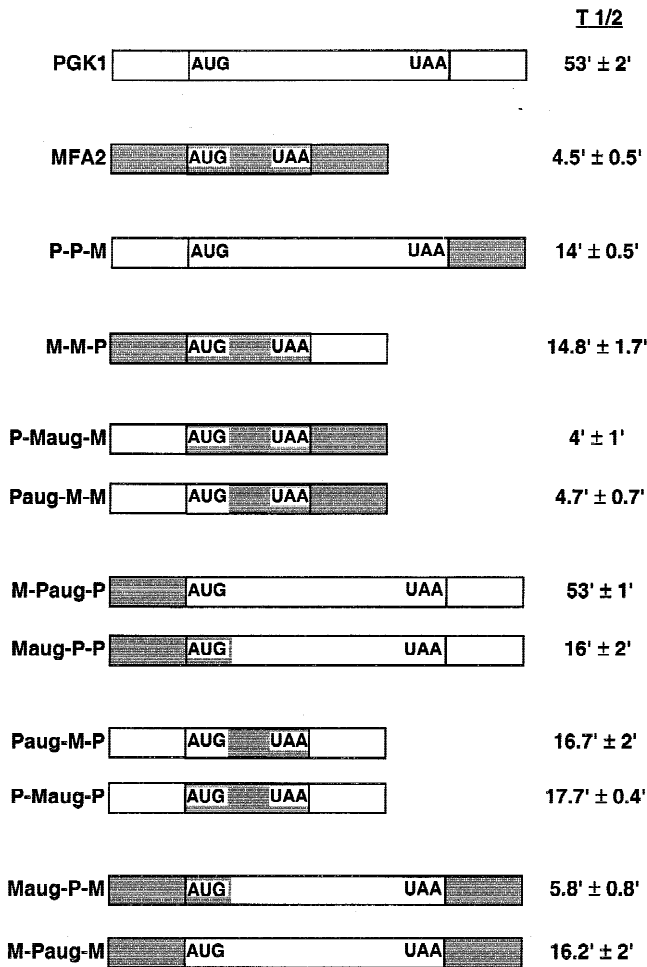
RESULTS

Experimental strategy

Genes encoding chimeric mRNAs consisting of various combinations of the 5' UTR, coding region, and 3' UTR of the MFA2 and PGK1 mRNAs were constructed as described in Materials and Methods. The chimeric mRNAs examined, listed in Figure 1, are designated by a three-letter nomenclature that indicates which parental mRNA contributed the 5' UTR, coding region, and 3' UTR of a particular transcript. The genes encoding these mRNAs were introduced into yeast strains on centromere plasmids and were expressed under control of the *GAL*1 upstream activating sequence (UAS). To measure mRNA decay rates we utilized a yeast strain that carried the temperature sensitive *rpb*1-1 allele of RNA polymerase II, thereby allowing repression of transcription by the simultaneous addition of dextrose (to cultures grown in galactose containing media at 24 °C) and shifting the cultures to 36 °C. The results obtained with the chimeric mRNAs are described below.

The role of the 3' UTRs

To test the role of the 3' UTR sequences, two constructs were made. First, we replaced the PGK1 3' UTR with the MFA2 3' UTR to generate the mRNA P-P-M. This transcript was approximately threefold less stable than the PGK1 mRNA (Fig. 2A) demonstrating that the MFA2 3' UTR was sufficient to accelerate the slow degradation of the PGK1 transcript, although not to the rate of the MFA2 transcript itself. The MFA2 3' UTR in this context was previously shown to increase the rate of deadenylation for the parental PGK1 mRNA, whereas the rate of decapping was unaffected (Decker & Parker, 1993).

Second, the 3' UTR of MFA2 was replaced with the PGK1 3' UTR to generate the mRNA designated M-M-P. This replacement caused the unstable MFA2 transcript to be stabilized approximately threefold (Fig. 2B). To determine the steps in mRNA decay affected by replacement of the MFA2 3' UTR, the decay of the M-M-P mRNA was examined in a transcriptional pulse-chase analysis, in which the *GAL*1 UAS is used to produce a synchronous pool of transcripts whose decay can be monitored for both deadenylation and subsequent decay (Decker & Parker, 1993). It should be noted that in

T 1/2

Transcript	T 1/2
PGK1	53' ± 2'
MFA2	4.5' ± 0.5'
P-P-M	14' ± 0.5'
M-M-P	14.8' ± 1.7'
P-Maug-M	4' ± 1'
Paug-M-M	4.7' ± 0.7'
M-Paug-P	53' ± 1'
Maug-P-P	16' ± 2'
Paug-M-P	16.7' ± 2'
P-Maug-P	17.7' ± 0.4'
Maug-P-M	5.8' ± 0.8'
M-Paug-M	16.2' ± 2'

FIGURE 1. The parental PGK1 and MFA2 mRNAs and the derived chimeric transcripts are schematically represented as boxes consisting of three parts that indicate the 5′ UTR, coding region, and 3′ UTR. The PGK1 sequences are shown as open boxes and the MFA2 sequences as shaded boxes. The three letter nomenclature of the chimeric mRNAs indicates the sequences of the 5′ UTR, coding region, and 3′ UTR, which are derived from the PGK1 (P) or MFA2 (M) transcripts. The lower case aug is used in the nomenclature to indicate the mRNA that contributed the context of the start codon. The natural 328-nt MFA2 transcript consists of 5′ UTR, coding region, and 3′ UTR sequences that are respectively 42, 117, and 169 nt long, whereas the natural 1,462-nt PGK1 transcript consists of 5′ UTR, coding region, and 3′ UTR sequences that are respectively 41, 1,251, and 170 nt long. The PGK1 coding region is depicted as longer than the MFA2 coding region to reflect the large difference in the lengths of the two coding regions. Half-lives are shown to the right of each transcript and were determined from the average of at least three experiments, as described in Materials and Methods.

the deadenylation-dependent decapping pathway of mRNA decay, the 5′-to-3′ exonucleolytic decay that follows decapping occurs at a much faster rate than either deadenylation or decapping (Muhlrad et al., 1994, 1995). We therefore interpret differences in postdeadenylation decay rates to reflect differences in rates of decapping. As shown in Figure 2C, the M-M-P mRNA had slower rates of deadenylation and decapping than the MFA2 mRNA. These stabilizing effects are indistinguishable from those obtained when the destabilizing
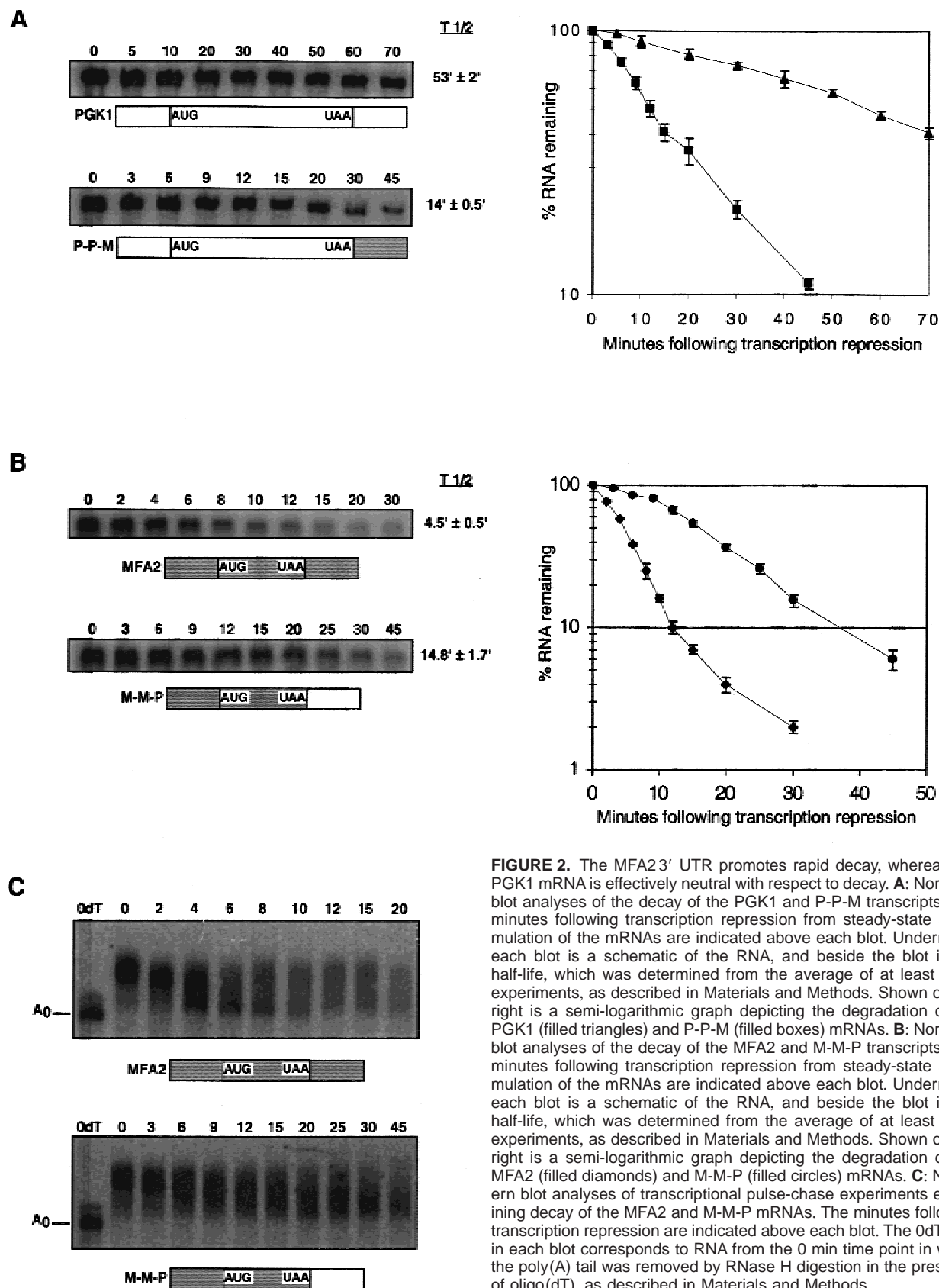
influence of MFA2 3′ UTR is neutralized by point mutations (Muhlrad & Parker, 1992; data not shown). We interpret these results to indicate that the PGK1 3′ UTR is neutral for mRNA decay rates and the stability of the PGK1 transcript must be due to other features of the transcript (see Discussion).

The role of the 5′ UTRs

Since mRNA decapping is a key step in the degradation of the MFA2 and PGK1 mRNAs, a reasonable hypothesis was that the sequence near the 5′ cap structure might play a role in specifying the rate of decapping. For example, the MFA2 5′ UTR might specify rapid decapping, while the PGK1 5′ UTR might dictate a slower rate of decapping. Given this possibility, we examined the 5′ UTRs of these mRNAs for effects on mRNA turnover. To test the PGK1 5′ UTR for potential stabilizing effects, two chimeric mRNAs that exchanged the MFA2 5′ UTR with the PGK1 5′ UTR were constructed (see Fig. 3). The first of these exchanged the majority of the 5′ UTR to yield the transcript P-Maug-M, where "aug" designates the mRNA that contributed the sequence context surrounding the start codon. Effects of the 5′ UTR on mRNA decay might require the native sequence context of the 5′ UTR and start codon, so a second chimeric mRNA designated Paug-M-M was constructed to fuse the PGK1 5′ UTR and first six codons to the fourth codon of the MFA2 coding region. Replacement of the MFA2 5′ UTR with that of PGK1, in either the P-Maug-M or Paug-M-M context, did not alter the rapid decay of the parental MFA2 transcript (Fig. 1 and data not shown). Furthermore, the decay profiles of the P-M-M mRNAs were determined to be the same as that of the parental MFA2 mRNA by transcriptional pulse-chase experiments (data not shown). We interpret these results to indicate that the MFA2 5′ UTR is not required for the rapid decapping of this transcript, and that the PGK1 5′ UTR, with or without the context of the PGK1 translation start codon, is not sufficient to specify a slower rate of decapping.

The reciprocal experiments, in which the PGK1 5′ UTR was replaced with the MFA2 5′ UTR yielded two mRNAs, M-Paug-P and Maug-P-P, that differed in their decay rates. Replacement of the majority of the PGK1 5′ UTR with the MFA2 5′ UTR in the M-Paug-P context did not affect decay of the parental PGK1 message, as judged by half-life determination (Fig. 4A) and transcriptional pulse-chase analysis (data not shown). These observations indicated that the MFA2 5′ UTR *per se* is not sufficient to accelerate mRNA decay, either by affecting decapping or deadenylation.

In contrast, the Maug-P-P mRNA, which contains the MFA2 5′ UTR and first three codons fused to the seventh codon of the PGK1 coding region (Fig. 3), was reproducibly approximately threefold less stable than the PGK1 mRNA (Fig. 4A). Interestingly, although the

FIGURE 2. The MFA2 3′ UTR promotes rapid decay, whereas the PGK1 mRNA is effectively neutral with respect to decay. **A**: Northern blot analyses of the decay of the PGK1 and P-P-M transcripts. The minutes following transcription repression from steady-state accumulation of the mRNAs are indicated above each blot. Underneath each blot is a schematic of the RNA, and beside the blot is the half-life, which was determined from the average of at least three experiments, as described in Materials and Methods. Shown on the right is a semi-logarithmic graph depicting the degradation of the PGK1 (filled triangles) and P-P-M (filled boxes) mRNAs. **B**: Northern blot analyses of the decay of the MFA2 and M-M-P transcripts. The minutes following transcription repression from steady-state accumulation of the mRNAs are indicated above each blot. Underneath each blot is a schematic of the RNA, and beside the blot is the half-life, which was determined from the average of at least three experiments, as described in Materials and Methods. Shown on the right is a semi-logarithmic graph depicting the degradation of the MFA2 (filled diamonds) and M-M-P (filled circles) mRNAs. **C**: Northern blot analyses of transcriptional pulse-chase experiments examining decay of the MFA2 and M-M-P mRNAs. The minutes following transcription repression are indicated above each blot. The 0dT lane in each blot corresponds to RNA from the 0 min time point in which the poly(A) tail was removed by RNase H digestion in the presence of oligo(dT), as described in Materials and Methods.

<u>T 1/2</u>

PGK1: 5′**AAGGAAGUAAUUAUCUACUUUUUACAACAGAUCUAAAAACA AUG UCU UUA UCU UCA AAG AUC UCU GUC**...3′ **53′ ± 2′**
 M   S   L   S   S   K   I   S   V

MFA2: 5′cagcgagcuaucaucuucauacaacaagaucuaccaaccuua aug caa cag auc ucc acu...3′ **4.5′ ± 0.5′**
 m   q   q   i   s   t

P-Maug-M: 5′**AAGGAAGUAAUUAUCUACUUUUUACAAC**agaucuaccaaccuua aug caa cag auc ucc acu...3′ **4′ ± 1′**
 m   q   q   i   s   t

Paug-M-M: 5′**AAGGAAGUAAUUAUCUACUUUUUACAACAGAUCUAAAAACA AUG UCU UUA UCU UCA AAG** auc ucc acu...3′ **4.7′ ± 0.7′**
 M   S   L   S   S   K i   s   t

M-Paug-P: 5′cagcgagcuaucaucuucauacaaca**AGAUCUAAAAACA AUG UCU UUA UCU UCA AAG AUC UCU GUC**...3′ **53′ ± 1′**
 M   S   L   S   S   K   I   S   V

Maug-P-P: 5′cagcgagcuaucaucuucauacaacaagaucuaccaaccuua aug caa cag **AUC UCU GUC**...3′ **16′ ± 2′**
 m   q   q   **I   S   V**

M-aug-P-P: 5′cagcgagcuaucaucuucauacaacaagaucuaccaaccuua **AUG UCU UUA UCU UCA AAG AUC UCU GUC**...3′ **36′ ± 4′**
 M   S   L   S   S   K   I   S   V

M-aug-M6P-P: 5′cagcgagcuaucaucuucauacaacaagaucuaccaaccuua aug caa cag auc ucc acu **AUC UCU GUC**...3′ **14.5′ ± 2.5′**
 m   q   q   i   s   t   **I   S   V**

M-aug-*P6P*-P: 5′cagcgagcuaucaucuucauacaacaagaucuaccaaccuua *AUG AGC CUU AGC AGU AAA* **AUC UCU GUC**...3′ **17′ ± 1′**
 M   S   L   S   S   K   I   S   V

FIGURE 3. The 5′ UTR and sequence contexts of the translational start codons of the PGK1, MFA2, and chimeric mRNAs are shown. The corresponding amino acids for each codon are shown below the RNA sequence. PGK1 sequences are represented as bold-face, upper case letters and MFA2 sequences are represented as plain, lower case letters. In the M-aug-<u>P</u>6P-P sequence, the different codons that encode the natural PGK1 amino acids are represented in upper case italics. The underlined regions indicate the *Bgl*II sites that were used to construct the chimeric genes, as described in Materials and Methods. Shown on the right of each sequence is the half-life of the transcript.

majority of the transcripts showed a faster decay rate, there was a residual pool of mRNAs that appeared to show slower decay for this construct. This possible bi-phasic decay formally raises the possibility that the effect of the AUG context is on an initial discriminatory event, which, if successfully completed, leads to a stable mRNA. Transcriptional pulse-chase analyses indicated that the differences in stability between the M-Paug-P and Maug-P-P mRNAs were due to changes in both the rates of deadenylation and decapping (Fig. 4B). Since the only difference between the M-Paug-P and Maug-P-P mRNAs is the sequence surrounding the translational start codon, these observations suggest that the context of the start codon can affect mRNA decay rates (see below).

The role of the coding regions

To examine the role of the MFA2 and PGK1 coding regions in the decay of the mRNAs, chimeric transcripts derived by exchanging the PGK1 and MFA2 coding regions were constructed. Since the results above suggested that the context of the translational start codon could influence mRNA decay rates, we constructed chimeras with or without an exchange of the translational start site. In one pair of constructs, we analyzed the effects of replacing the PGK1 coding region with the MFA2 coding region, which yielded the Paug-M-P and P-Maug-P mRNAs. These were both moderately stable mRNAs that were approximately

threefold less stable than the PGK1 mRNA (Fig. 5A). Notably, the decay rates of the Paug-M-P and P-Maug-P mRNAs were nearly identical to that of the M-M-P transcript (Fig. 2B), indicating that the PGK1 5′ UTR with or without the context of its native translational start codon has no effect on the degradation rate when fused to the MFA2 coding region.

In the reciprocal set of constructs, the MFA2 coding region was replaced with the PGK1 coding region in the Maug-P-M and M-Paug-M contexts. The Maug-P-M transcript was unstable and similar to the MFA2 mRNA in stability. This observation indicated that the MFA2 coding region was not required for rapid mRNA degradation. In contrast, the M-Paug-M transcript was stabilized approximately threefold relative to the MFA2 mRNA (Fig. 5B). This observation suggests that the PGK1 coding region contains features that promote mRNA stability (see Discussion). However, because the only difference between the M-Paug-M and Maug-P-M mRNAs is the sequence surrounding the translational start codon, these observations argued that the ability of the PGK1 coding region to stabilize an mRNA required that the translation start codon be in the PGK1 sequence context. The MFA2 coding region appears to be insensitive to the context of the start codon, since the Paug-M-P and P-Maug-P mRNAs have similar stabilities. We conclude that the PGK1 mRNA is stabilized by an effect that requires both the context of the PGK1 start codon and sequences from within the coding region.
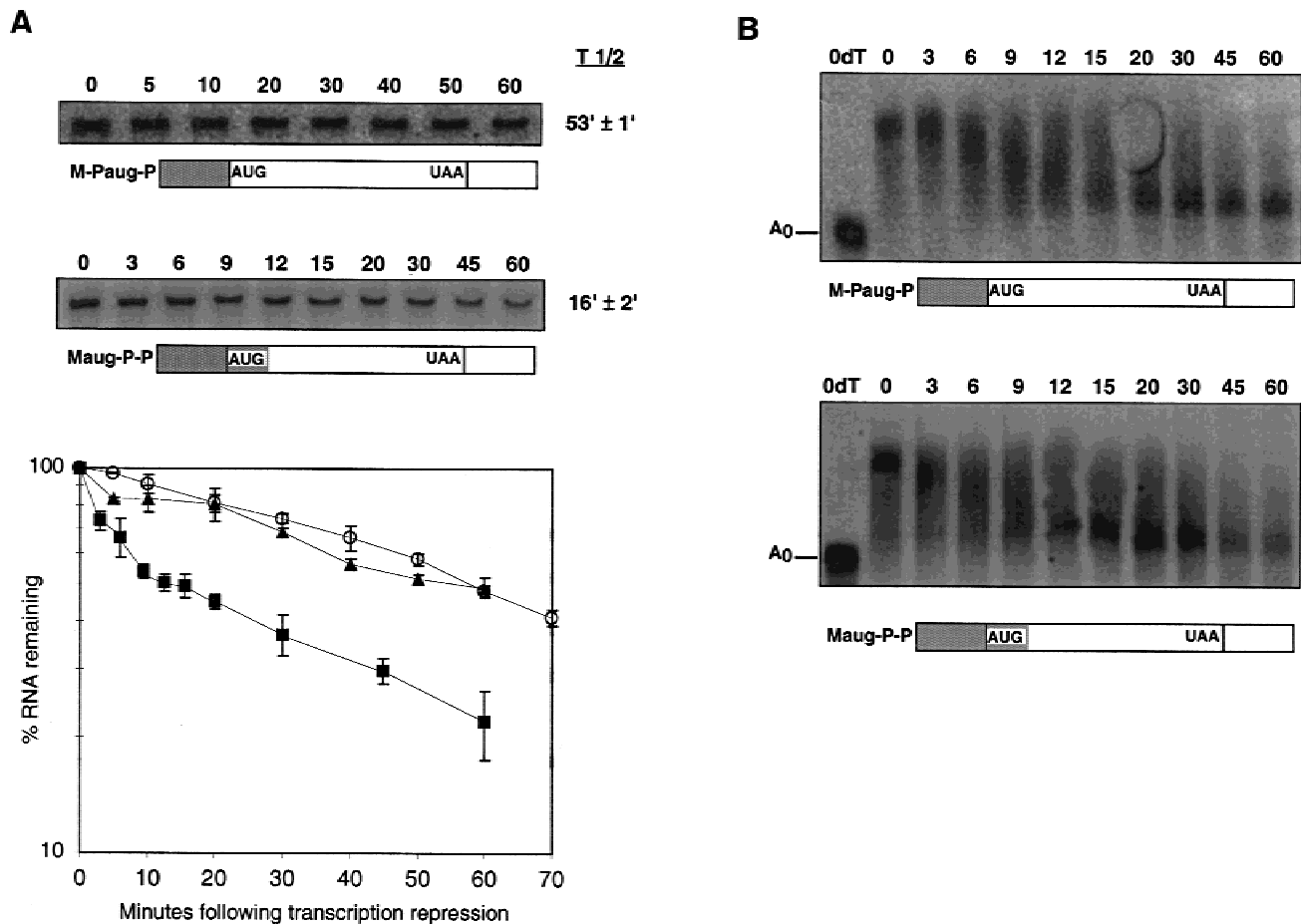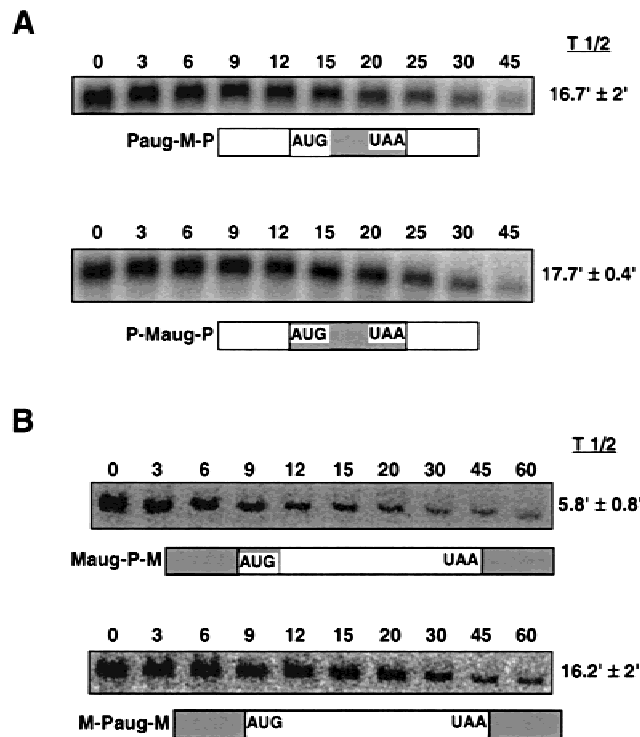
FIGURE 4. The context of the PGK1 start codon can affect mRNA decay. **A:** Northern blot analyses of the decay of the M-Paug-P and Maug-P-P transcripts. The minutes following transcription repression from steady-state accumulation of the mRNAs are indicated above each blot. Underneath each blot is a schematic of the RNA, and to the right is the half-life, which was determined from the average of at least three experiments, as described in Materials and Methods. A semi-logarithmic graph depicting the degradation of the PGK1 (open circles), M-Paug-P (filled triangles), and Maug-P-P (filled boxes) transcripts is shown below the Northern blots. **B:** Northern blot analyses of transcriptional pulse-chase experiments examining decay of the M-Paug-P and Maug-P-P mRNAs. The minutes following transcription repression are indicated above each blot. The 0dT lane in each blot corresponds to RNA from the 0 min time point in which the poly(A) tail was removed by RNase H digestion in the presence of oligo(dT), as described in Materials and Methods.

The native context of the start codon is required for the stabilizing influence of the PGK1 coding region

An important issue is what feature of the context of the PGK1 start codon affects mRNA decay rates. Comparison of the M-Paug-P and Maug-P-P mRNAs sequences (see Fig. 3) suggests three possible explanations. First, since the exact number of codons between the translation start codon and the PGK1 coding region differ in these mRNAs, the spacing between the translation start and some important region of the PGK1 coding region could be affecting decay changes. Second, changes in the RNA sequence itself surrounding the start codon might alter a property of the mRNA and thereby affect mRNA degradation. Alternatively, the effect of the context could be due to changes in the nascent PGK1

peptide on the stability of the transcript. This latter possibility is raised by the observations that the sequence of the nascent peptide can affect the stability of the mammalian β-tubulin transcript (Gay et al., 1989).
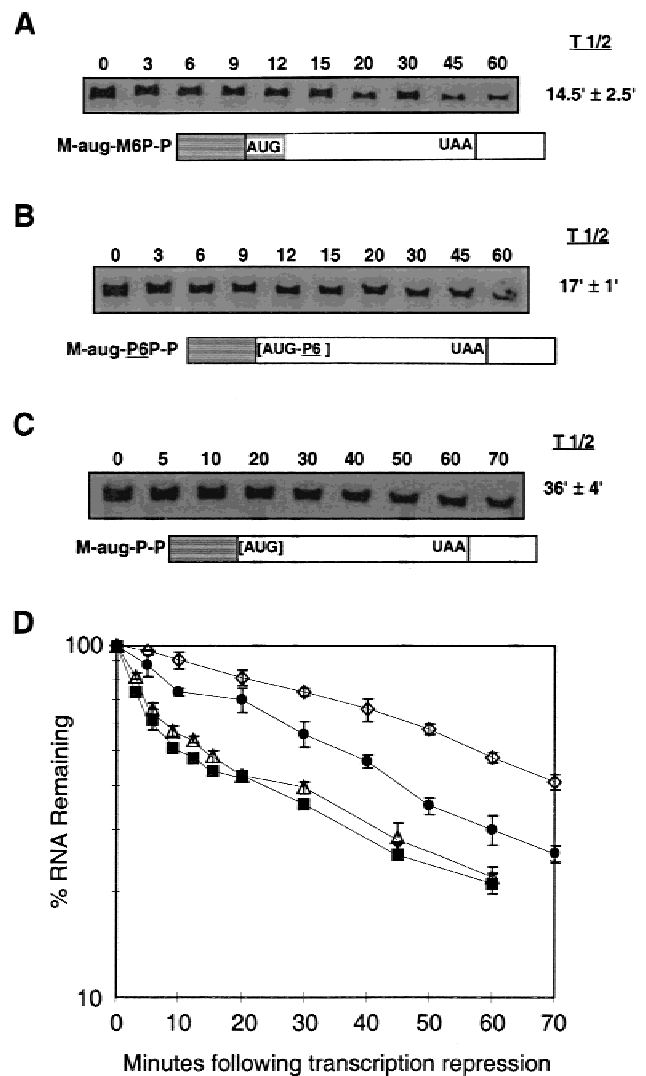
To address whether the change in codon number between the translation start site and the PGK1 coding region might affect decay, we examined the decay of the Maug-M6P-P chimeric mRNA. This transcript contained the MFA2 5′ UTR and first 6 codons fused to codon 7 of the PGK1 coding region, whereas the Maug-P-P construct replaced the PGK1 5′ UTR and codons 1–6 with the MFA2 5′ UTR and codons 1–3 (Fig. 3). The Maug-M6P-P mRNA (Fig. 6A) was similar in stability to the Maug-P-P mRNA, indicating that the Maug-P-P mRNA is not less stable than the PGK1 mRNA because of the spacing of the start codon relative to the PGK1 coding region.

A

Paug-M-P   T 1/2 = 16.7' ± 2'

P-Maug-P   T 1/2 = 17.7' ± 0.4'

B

Maug-P-M   T 1/2 = 5.8' ± 0.8'

M-Paug-M   T 1/2 = 16.2' ± 2'

FIGURE 5. The PGK1 coding region acts as a stabilizing element, provided that the natural context of the PGK1 start codon is present. Northern blot analyses of the decay of the Paug-M-P and P-Maug-P transcripts (**A**) and the Maug-P-M and M-Paug-M transcripts (**B**). The minutes following transcription repression from steady-state accumulation of the mRNAs are indicated above each blot. Underneath each blot is a schematic of the RNA, and to the right is the half-life, which was determined from the average of at least three experiments, as described in Materials and Methods.

To test if the effect of the sequence changes surrounding the AUG start codon was potentially due to changes in the nascent peptide, we examined the decay of the M-aug-P6P-P mRNA. This transcript contains the MFA2 5′ UTR fused to a PGK1 coding region in which the first six codons were replaced with a different RNA sequence that encodes the same amino acids. The decay rate of this mRNA (Fig. 6B) was similar to that of the Maug-P-P mRNA and was approximately threefold less stable than the PGK1 or M-Paug-P transcripts. This observation demonstrated that the effect of altering the sequence surrounding the start codon was due to changes in the RNA sequence, and that nucleotides 3′ of the AUG codon were required for the stabilizing effect of the PGK1 coding region.

We next examined whether the stabilizing effect of the PGK1 start codon and coding region requires any specific sequences 5′ of the AUG. To determine whether changes 5′ of the start codon could contribute to changes in stability of the PGK1 mRNA, we fused the entire MFA2 5′ UTR to the PGK1 coding region precisely at the AUG codon, so that the PGK1 sequence 3′ of the start codon is unaltered. The M-aug-P-P tran-

A

M-aug-M6P-P   T 1/2 = 14.5' ± 2.5'

B

M-aug-P6P-P [AUG-P6] UAA   T 1/2 = 17' ± 1'

C

M-aug-P-P [AUG] UAA   T 1/2 = 36' ± 4'

D

FIGURE 6. The PGK1 mRNA is stabilized by the native context of the start codon and the coding region. Northern blot analyses of the decay of the M-aug-M6P-P (**A**), M-aug-P6P-P (**B**), and M-aug-P-P (**C**) transcripts. The M-aug-M6P-P transcript has the MFA2 5′ UTR and first 6 codons fused to codon 7 of the PGK1 mRNA, as illustrated in Figure 3. The M-aug-P6P-P mRNA contains the MFA2 5′ UTR precisely fused to the start codon of a PGK1 mRNA derivative in which the first 6 codons (indicated in italics in Fig. 3) were replaced with different sequence that encodes the same amino acids. The M-aug-P-P transcript contains the MFA2 5′ UTR fused precisely to the PGK1 start codon, in contrast to the Maug-P-P transcript (see Fig. 3). The minutes following transcription repression from steady-state accumulation of the mRNAs are indicated above each blot. Underneath each blot is a schematic of the RNA, and to the right is the half-life, which was determined from the average of at least three experiments, as described in Materials and Methods. **D**: A semi-logarithmic graph depicting the degradation of the M-aug-M6P-P (filled boxes), M-aug-P6P-P (open triangles), M-aug-P-P (filled circles), and PGK1 (open diamonds) mRNAs.

script had a half-life of 36 min (Fig. 6C), which was intermediate between the M-Paug-P ($t_{1/2}$ = 53 min) and Maug-P-P ($t_{1/2}$ = 16 min) mRNAs. The slight, but reproducible, decrease in stability of the M-aug-P-P construct compared to the PGK1 mRNA indicated that

the PGK1 coding region requires some native sequence 5′ of the start codon for its maximal stabilizing effect. This observation, in combination with the above results, indicated that RNA sequences both 5′ and 3′ of the PGK1 AUG, or essentially the PGK1 AUG sequence context, were required for the maximal stabilizing effect of this region.

Changes in the context of the PGK1 start codon affect both the stability and the translational efficiency of the message

The observation that the sequence context of the PGK1 translation start codon affected mRNA turnover was unexpected and raised the issue as to how this particular region might affect decay rate. Prior work from a variety of eukaryotes has demonstrated that alterations in the context of the translation start codon can affect the efficiency of translation initiation (Merrick & Hershey, 1996). For example, in yeast cells, alterations of the initiator region surrounding the start codon of the HIS4 (Cigan et al., 1988), CYC1 (Baim & Sherman, 1988), and CYC7 (Yun et al., 1996) mRNAs decrease the efficiency of translation approximately 40%. These observations suggested the hypothesis that the PGK1 start codon context and/or the PGK1 coding region were influencing both the rate of translation initiation and mRNA turnover, perhaps in a coordinate manner. A critical test of this hypothesis is that the alterations which affect mRNA decay rate should also affect the translation efficiency of the mRNA. To examine this possibility two experiments were performed.

As a first experiment to determine if changing the PGK1 start codon context also affected translation efficiency, we compared the polysome gradient distribution of the PGK1 mRNA as compared to a PGK1 mRNA with an altered context around the start codon. To allow subsequent comparison of protein activity (see below) we utilized the M-aug-P6P-P chimera as the mRNA with an altered PGK1 start codon context. If the alteration of the PGK1 start codon reduced the translation efficiency of the transcript then it would be expected that the chimeric transcript would have fewer ribosomes per mRNA. The distribution of the chimeric transcript in a sucrose density polysome profile should therefore be shifted towards the lighter fractions as compared to the PGK1 mRNA distribution. To avoid potential artifacts in polysome distributions we performed our analysis in the absence of cycloheximide, which can drive additional mRNAs into the polysome bound pool (see Atkin et al., 1995).

An important result was that the distribution of the M-aug-P6P-P chimera in the polysome gradient was altered in two manners consistent with a decrease in its translational efficiency. First, in contrast to the wild-type PGK1 mRNA control, a significant amount of the M-aug-P6P-P chimera was found in the fractions lighter than the 80S peak indicating transcripts that were not even being translated (compare Fig. 7B,C and 7E,F). In addition, the transcripts that were found within the polysome portion of the gradient were shifted towards lighter polysomes (compare Fig. 7B,C and 7E,F). While the A254 profiles of the two independent yeast cultures were similar (Fig. 7A,C), as a control we examined the profiles for their distribution of the CYH2 mRNA and found them to be essentially identical (Fig. 7B,D). These observations argued that the alteration of the PGK1 start codon occurring in the M-aug-P6P-P chimera, which accelerated mRNA decay rate, also inhibited the translation efficiency of the mRNA.

The second experiment we performed to address whether changes in the context of the PGK1 start codon altered the translational efficiency of the mRNA was to compare the relative translational efficiency of the PGK1-lacZ and M-aug-P6P-lacZ fusion transcripts by determining the β-galactosidase activity produced as standardized to mRNA levels. We utilized the latter transcript in this experiment for two reasons. First, changes in the sequence context of the PGK1 start codon in the M-aug-P6P-P chimera caused loss of the stabilizing influence of the PGK1 AUG context (see above). Second, the M-aug-P6P-lacZ mRNA encodes the same fusion peptide as the PGK1-lacZ fusion; thus any differences in enzymatic activity would not be because of a difference in the specific activity, or stability, of the fusion protein.

We first examined the relative stabilities of the PGK1-lacZ and M-aug-P6P-lacZ fusion transcripts. As shown in Figure 8A, the M-aug-P6P-lacZ mRNA ($t_{1/2}$ = 5.8 min) was less stable than the PGK1-lacZ transcript ($t_{1/2}$ = 10 min), which was consistent with a loss of the PGK1 stabilizing effect in the M-aug-P6P-lacZ transcript. Both of these PGK1-lacZ fusion transcripts were less stable than the parental PGK1 mRNAs, presumably because of destabilizing features contributed by the lacZ coding regions. Despite the differences in their half-lives, the PGK1-lacZ and M-aug-P6P-lacZ transcripts accumulated to the same relative steady-state levels (Fig. 8A). This is a reproducible result and argues that the steady-state levels of these mRNAs therefore appear to be determined not only by their rates of decay, but by additional, unknown aspects of their metabolism.

A critical observation was that the M-aug-P6P-lacZ mRNA was observed to be translated less efficiently than the PGK1-lacZ fusion transcripts. The M-aug-P6P-lacZ transcript produced nearly five times less β-galactosidase activity per mRNA level than did the PGK1-lacZ transcript (Fig. 8A). This observation, and the altered polysome distribution of the M-aug-P6P-P chimera, indicated that the sequence context of the PGK1 start codon has a significant effect on the translational efficiency of the transcript.
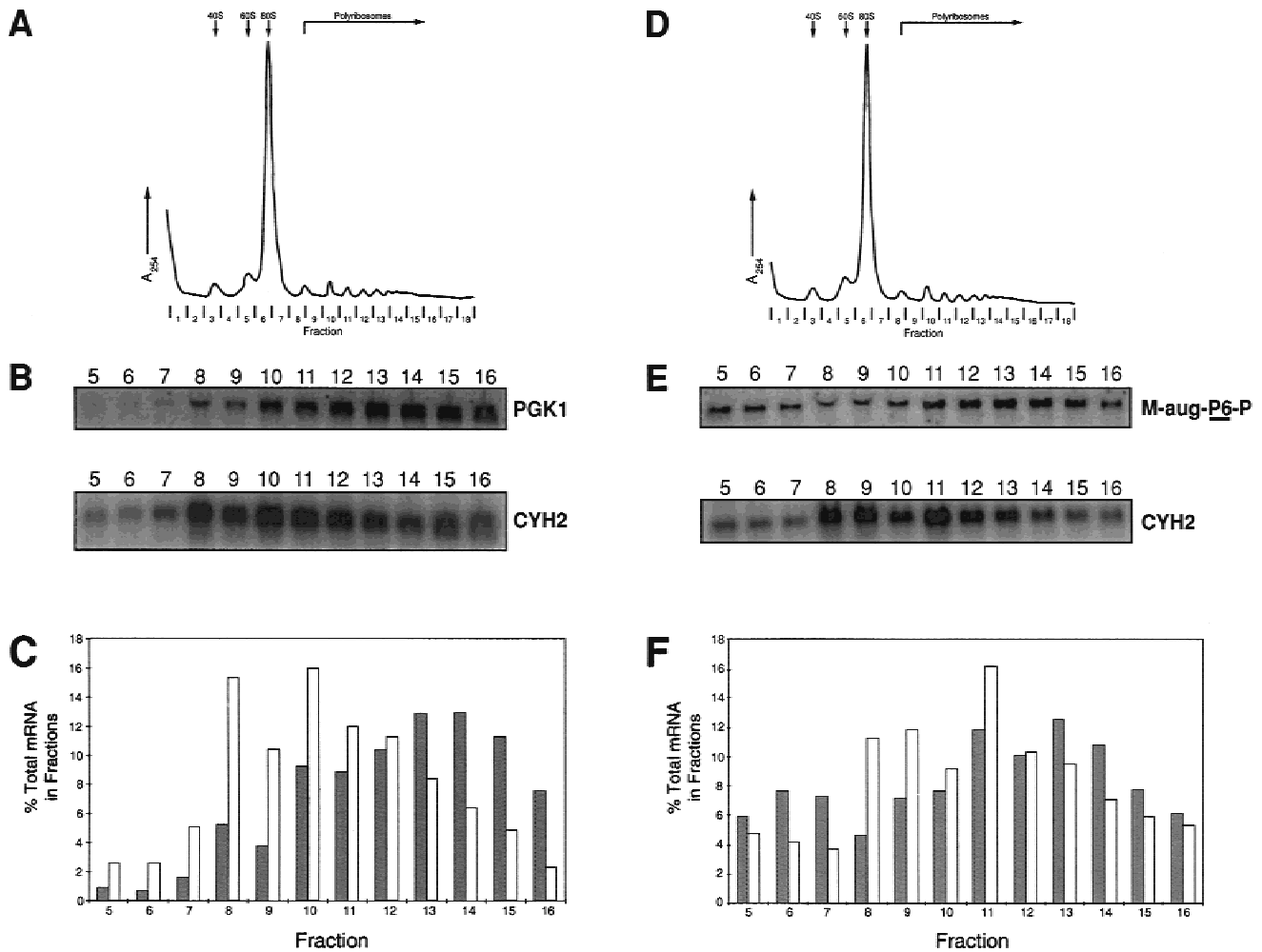
FIGURE 7. Changes in the context of the PGK1 start codon affect the polysome distribution of the mRNA. **A,D:** Polysome profiles from cells expressing either the PGK1 mRNA (**A**) or the M-aug-P6P-P mRNA (**D**). Cytoplasmic extracts were prepared and fractionated on sucrose gradients as described in Materials and Methods. The OD tracings (measured by OD254) of the gradients are shown and the positions of the 40S, 60S, and 80S, and polyribosome peaks are indicated by arrows. Fractions from the gradients are indicated below the OD tracings. **B:** Northern blot analysis of the distribution of the PGK1 and CYH2 mRNAs from the PGK1 polysome profile shown in **A**. **C:** Histogram showing the distribution of the PGK1 (filled bars) and the CYH2 (open bars) mRNAs from the Northern blot analysis in **B**. The amount of mRNA is each fraction is expressed as a percentage of the total amount of mRNA detected in all of the fractions (5–16) combined. **E:** Northern blot analysis of the distribution of the M-aug-P6P-P and CYH2 mRNAs from the PGK1 polysome profile shown in **D**. **F:** Histogram showing the distribution of the M-aug-P6P-P (filled bars) and the CYH2 (open bars) mRNAs from the Northern blot analysis in **E**. The amount of mRNA is each fraction is expressed as a percentage of the total amount of mRNA detected in all of the fractions (5–16) combined.
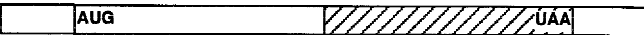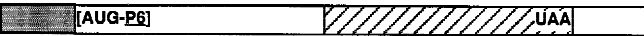
Interaction of the PGK1 start codon context and the coding region

The above results suggested two general possibilities as to why the stability of the PGK1 mRNA requires both the sequence context of the PGK1 start codon and the coding region. One possibility is that the context of the start codon promotes efficient translation of the PGK1 mRNA, which in turn could be required for the PGK1 coding region to function as a stabilizing element. In this model, the effect of the translation start site on translation efficiency should be independent of the PGK1 coding region. An alternative model is that the coding region might function to promote efficient translation of the PGK1 mRNA in a manner that requires the native sequence context of the start codon. In this second view, deletion of the coding region should reduce the translational efficiency of the mRNA as compared to a full-length fusion transcript, and the differences between the sequence contexts of the start codon should be minimized.

To distinguish between these possibilities, we examined the translational efficiency of the chimeric PGK1Δ81-lacZ and M-aug-P6PΔ81-lacZ transcripts. These transcripts were derived from the PGK1-lacZ and M-aug-P6P-lacZ transcripts by deleting the 3′ 81%

A

	T 1/2	Steady state RNA level	% Relative ß-gal activity per RNA level
PGK1-lacZ	10' ± 2'	1	100
M-aug-P6P-lacZ	5.8' ± 1.2'	0.98	21.2 ± 0.5

B

PGK1Δ81-lacZ	9.5' ± 0.5'	0.76	18.4 ± 0.7
M-aug-P6PΔ81-lacZ	9' ± 2'	0.82	10.5 ± 0.8

FIGURE 8. Changes in the context of the PGK1 start codon affect the translational efficiency of the transcript as assessed by protein produced per mRNA level. **A**: The PGK1-lacZ and M-aug-P6P-P fusion mRNAs are schematically represented as boxes in which the PGK1 sequences are shown as open boxes, the lacZ sequences as striped boxes, and the MFA2 sequences as shaded boxes. The half-life of each mRNA was determined from the average of three experiments. The steady-state level of each mRNA for the β-galactosidase expression assays was determined by Northern blot analysis from two experiments as described in Materials and Methods and is normalized to the amount of PGK1-lacZ mRNA. The percent relative β-galactosidase activity was determined from at least two experiments in which the amount of activity was adjusted to reflect the relative steady-state level of each mRNA. The relative β-galactosidase activity per RNA is expressed as a percentage of the PGK1-lacZ activity level. **B**: The PGK1Δ81-lacZ and M-aug-P6PΔ81-P fusion mRNAs are schematically represented as described above. Half-lives and steady-state levels of the RNAs were determined as described above and are normalized to the amount of PGK1Δ81-lacZ mRNA. The percent relative β-galactosidase activity (determined as above) per RNA is expressed as a percentage of the PGK1Δ81-lacZ activity level.

of the PGK1 coding region. A similar deletion was previously shown to destabilize the parental PGK1 mRNA approximately twofold (Heaton et al., 1992), and thereby inactivate the stabilizing influence of the PGK1 coding region. Comparison of the PGK1Δ81-lacZ and M-aug-P6PΔ81-lacZ transcripts was therefore anticipated to provide a means of assessing the effect of changes in the context of the PGK1 start codon on translational efficiency, without influence from the PGK1 coding region.

The PGK1Δ81-lacZ and M-aug-P6PΔ81-lacZ transcripts were determined to have nearly identical half-lives and steady-state mRNA levels (Fig. 8B). The steady-state levels were also essentially the same as those seen for the full-length PGK1-lacZ fusion transcripts (Fig. 8). The translational efficiencies of the PGK1Δ81-lacZ and M-aug-P6PΔ81-lacZ mRNAs differed less than twofold, as judged by β-galactosidase activity per mRNA level (Fig. 8B). In contrast, the translational efficiencies of the parental full-length PGK1-lacZ fusion constructs differed nearly fivefold (Fig. 8A). These observations argued that the larger translational difference seen with the full-length constructs was dependent on the coding region. The PGK1 coding region could therefore stabilize the mRNA by promoting efficient translation initiation in a manner that is dependent on the sequence context of the AUG. Consistent with a role of the PGK1 coding region in promoting translation, the translational efficiency of the PGK1Δ81-lacZ mRNA was also reduced compared to that of the full

length PGK1-lacZ transcript (Fig. 8). Because the PGK1-lacZ and PGK1Δ81-lacZ transcripts produce different polypeptides, however, we cannot rule out the formal possibility that the differences in β-galactosidase levels from these transcripts could reflect differences in protein stability or specific activity of the fusion polypeptide. We interpret these results to suggest that the set of sequences that stabilize the PGK1 transcript also function to promote efficient translation, implying a coordinate link between translation and mRNA deadenylation and decapping (see Discussion).

DISCUSSION

Sequences that determine the differential decay of the MFA2 and PGK1 mRNAs

The role of the 3' UTRs

Our analysis of the MFA2 and PGK1 mRNAs has led to an understanding of the distribution of sequences that specify the different mRNA decay rates of these transcripts. One region of importance in determining the difference in decay of these mRNAs is the 3' UTR. Several lines of evidence both from this work and from previous experiments indicate that the MFA2 3' UTR contains sequences necessary for rapid mRNA degradation and sufficient to promote increased rates of degradation. First, replacement of the MFA2 3' UTR with the PGK1 3' UTR led to an increase in stability

(Fig. 2B). Similarly, point mutations or deletions within the MFA2 3′ UTR also stabilize the MFA2 transcript (Muhlrad & Parker, 1992). In addition, replacement of the PGK1 3′ UTR with the MFA2 3′ UTR led to an increase in the rate at which the PGK1 transcript was degraded (Fig. 2A), primarily because of an increase in the rate of deadenylation (Decker & Parker, 1993). Our data also argue that the PGK1 3′ UTR is effectively neutral with regards to affecting mRNA decay as, when attached to the MFA2 mRNA, the PGK1 3′ UTR behaved identically to the MFA2 3′ UTR in which the destabilizing element had been inactivated by mutations (Fig. 2B and unpubl. observations). Thus the 3′ UTR sequences contribute to the rapid decay of the MFA2 mRNA, but in the case of the stable PGK1, the role of the 3′ UTR is functionally neutral, thereby allowing other features of the transcript to specify its slow rate of decay.

The role of 5′ UTRs

Several observations lead to the conclusion that the 5′ UTR sequences *per se* do not influence the decay rate of either the PGK1 or MFA2 transcripts. The important observation was that reciprocal exchanges of the 5′ UTR between these mRNAs had no effect on mRNA decay rates (Figs. 1 and 6A), provided that the context of the translation start codon was left intact (see below). The implication of these results is that the local sequence adjacent to the cap structure is not a major determinant of the decapping rate for the MFA2 and PGK1 mRNAs. However, 5′ UTR sequences have been observed to promote rapid decay in the PPR1 (Pierrat et al., 1993), Ip (Cereghino & Scheffler, 1995), and OLE1 yeast mRNAs (Gonzalez & Martin, 1996). Whether these sequences influence rates of deadenylation, decapping, or both remains unknown. Thus, while 5′ UTRs may not generally influence rates of deadenylation or decapping, they can significantly influence the decay of particular transcripts.

The coding region and the context of the translation start codon

Our data suggest that the PGK1 coding region and the sequence context of the PGK1 translation start codon combine to stabilize the PGK1 transcript. The critical observation was that any transcript that contains the combination of these two regions was more stable than a comparable construct lacking either the context of the PGK1 start codon or the PGK1 coding region. The requirement for the context of the PGK1 start codon is illustrated by the Maug-P-P transcript ($t_{1/2}$ = 16 min) being threefold less stable than the M-Paug-P transcript ($t_{1/2}$ = 53 min) because of the change of the AUG context (Fig. 4A). Similarly, the Maug-P-M transcript ($t_{1/2}$ = 5.8 min) is approximately threefold less stable than the M-Paug-M mRNA ($t_{1/2}$ = 16 min, Fig. 5B). The

loss of stability seen without the PGK1 start codon can be attributed to a stabilizing effect from the PGK1 sequences, and not a destabilizing effect of the MFA2 start codon and coding region, because alteration of the AUG context to a novel sequence (M-aug-P6P-P) also destabilizes the transcripts (Fig. 6). Moreover, because the M-aug-P6P-P construct changed the RNA sequence around the translation start codon, without affecting the encoded protein, and inactivated the stabilizing effect of the PGK1 translation start region, we conclude that it is the RNA sequence of this region that is important for the stability of the transcript.

The ability of the PGK1 translation start codon context to affect turnover requires the presence of the PGK1 coding region. The critical observation was that constructs without the PGK1 coding region were less stable than comparable constructs with the PGK1 coding region. Moreover, constructs without the coding region showed essentially no change in mRNA decay rate in response to a change in the AUG context (compare P-Maug-M and Paug-M-M, Fig. 3; P-Maug-P and Paug-M-P, Fig. 5A). Thus, both the PGK1 coding region and the translation start codon act together to increase the stability of this mRNA.

The basis for the differential decay of the MFA2 and PGK1 transcripts

The summation of this work allows us to understand the sequences responsible for the differential decay of the MFA2 and PGK1 mRNAs. Our results indicate that the rapid decay of the MFA2 mRNA can be attributed to specific sequences within the 3′ UTR that promote rapid deadenylation and decapping. In contrast, the slow decay rate of the PGK1 mRNA can be attributed to the absence of sequences promoting mRNA degradation in its 3′ UTR and a stabilizing effect due to the context of the translation start codon and the PGK1 coding region. Thus, the decay rates of these mRNAs are modulated both by positive and negative influences from an intermediate rate of turnover. An important issue then is to determine how these sequences function to ultimately modulate mRNA deadenylation or decapping.

The interconnection between translation and mRNA turnover

Two observations demonstrated that the PGK1 start codon context and coding regions, which lead to stabilization of the mRNA, also promote efficient translation. First, the chimeric transcript M-aug-P6-P-P was found both in the nonpolysome fractions and was distributed in lighter polysomes as compared to the control PGK1 mRNA, which was essentially all found in polysomes (Fig. 7). Second, we observed (Fig. 8) that a reporter transcript containing both the PGK1 start codon context and the PGK1 coding region (PGK1-

lacZ) produced approximately 4–5 times more protein per mRNA as compared to a transcript where the PGK1 start codon context was altered (M-aug-P6P-lacZ). Similar results were seen with deletions of the PGK1 coding region (compare PGK1-lacZ to PGK1Δ81-lacZ). However, given that the fusion proteins compared in this latter case differ, caution must be used because the differences in activity could formally also reflect difference in specific activity or protein stability.

One surprising aspect of these experiments was that the PGK1 coding region was required for the full effect of the AUG context on translational efficiency. In the absence of the PGK1 coding region, changes to the AUG context yielded a modest twofold effect on translational efficiency (Fig. 8), similar to that previously seen for the yeast HIS4 (Cigan et al., 1988), CYC1 (Baim & Sherman, 1988), and CYC7 (Yun et al., 1996) mRNAs. These observations argue that the translational efficiency of the PGK1 transcript is not simply controlled by the sequence context of the PGK1 start codon, but rather that the PGK1 translational start and coding regions function together in promoting efficient translation of the PGK1 transcript.

The observation that the mRNA features that stabilize the PGK1 transcript also increase the efficiency of translation leads us to consider the mechanistic relationship between translation and mRNA degradation. Since the discovery that mRNA decapping is a key step in mRNA degradation, and that poly(A) tails are negative regulators of decapping, it has been proposed that mRNA decapping and translation initiation are in competition, although additional data in support of this hypothesis has not emerged. A strong prediction of this view, however, is that specific sequences that promote mRNA decapping will inhibit translation, whereas sequences that inhibit mRNA decapping will promote efficient translation. Consistent with this view, we observed that the PGK1 sequences that stabilize the mRNA also function to promote efficient translation. This interpretation is also consistent with previous results wherein completely blocking translation of the PGK1 mRNA by insertion of a strong secondary structure into its 5′ UTR promoted rapid mRNA degradation, although the extreme nature of this inhibition limited the conclusions that could be drawn from it (Muhlrad et al., 1995). Based on the above logic it is reasonable to propose that most, if not all, mRNA sequences or features that modulate mRNA decapping will also inversely modulate translation rate. For example, we predict that the 3′ UTR of the MFA2 mRNA will repress translation rate. Moreover, it is striking to note that the AU rich elements that promote mRNA decay in mammalian cells also function to inhibit translation initiation (Kruys & Huez, 1994), although it is not yet known if these sequences promote mRNA decapping.

The actual mechanistic relationship between the translational efficiency and degradation rate of the PGK1 mRNA is therefore a critical issue. The simplest possibility is that the rates of translation and degradation are determined by the assembly and disassembly of translation initiation factors on the cap structure and 5′ end of the mRNA, and that specific stages in this dynamic process have different susceptibility to decapping. In this light, it is interesting that for the stability of the PGK1 mRNA it is the context of the translational start site that is significant. A likely role for this region in promoting translation initiation would be to accelerate hydrolysis of GTP by eIF2, thereby allowing 60S joining and entry into the elongation phase of translation. This argues that steps late in the translation initiation process are required to prevent mRNA decapping, and that decapping is not simply controlled by proteins which interact with the 5′ cap structure itself such as the eIF-4F cap binding complex. This view is also consistent with observations that blocking translation initiation by mutations in eIF4F or eIF3 components gave accelerated decay (D. Schwartz & R. Parker, in prep.), whereas inhibition of elongation, either by the addition of cycloheximide (Herrick et al., 1990; Beelman & Parker, 1994) or by mutation of the CCA1 gene (Peltz et al., 1992) stabilizes mRNAs.

MATERIALS AND METHODS

Strain

The yeast strain used for these studies was yRP693 (Mat**a**, *rpb1-1*, *ura3-52*, *leu2-3, 112*). The gene of each mRNA studied was carried on a *cen*-plasmid, and expression was regulated by the *GAL*1 UAS. The plasmids were transformed into the yeast strain using standard techniques, and were maintained by growth in selective medium.

Plasmids

The mRNAs examined were expressed from the following plasmids: PGK1, pRP469; MFA2, pRP485; P-P-M, pRP430; M-M-P, pRP592; P-Maug-M, pRP593; Paug-M-M mRNA, pRP617; M-Paug-P, pRP594; P-Maug-P, pRP640; Paug-M-P, pRP641; M-Paug-M, pRP638; Maug-P-M, pRP639; M-aug-P-P, pRP711; M-aug-P6P-P, pRP712; M-aug-M6P-P, pRP713. The plasmids RP469, RP485, and RP430 have been previously described (Decker & Parker, 1993). The plasmid RP592 was constructed by ligating the *Bgl*II-*Hin*dIII fragment of pRP469 into the vector backbone of *Bgl*II-*Hin*dIII-digested pRP485. The plasmid RP593 was constructed in two steps. First, pRP539 was created by placing the *Sac*I-*Hin*dIII fragment of pRP455 (Muhlrad et al., 1994) into *Sac*I-*Hin*dIII-digested pRP410 (Decker & Parker, 1993). The *Bgl*II-*Hin*dIII fragment of pRP539 was in turn ligated to *Bgl*II-*Hin*dIII-digested pRP549 (Muhlrad et al., 1995), to yield pRP593. The plasmid RP617 was constructed in three steps. First, a *Bgl*II site was introduced into the MFA2 gene 4 nt downstream of the start codon in pRP493 (Muhlrad et al., 1994) by site-directed mutagenesis, using the oligonucleotide 5′-AGCAGTGGAGATCTGTTGCATT-3′ (oRP146) to create

pRP457. Second, the *Sac*I-*Hin*dIII fragment of pRP457 was ligated to *Sac*I-*Hin*dIII cut pRP410 (Decker & Parker, 1993) to create pRP615. Finally, the *Bgl*II-*Hin*dIII fragment of pRP615 was ligated to *Bgl*II-*Hin*dIII-digested pRP599 (Muhlrad et al., 1995) to yield pRP617. The plasmid RP594 was constructed by inserting a *Bgl*II-*Hin*dIII partial fragment of pRP549 (Muhlrad et al., 1995) into the plasmid backbone of *Bgl*II-*Hin*dIII-digested pRP539. The plasmid RP618 was assembled by ligating the *Bgl*II-*Hin*dIII fragment of pRP599 (Muhlrad et al., 1995) to *Bgl*II-*Hin*dIII-digested pRP615. To construct pRP640, the PGK1-MFA2 gene fragment from pRP593 was amplified with PCR using the oligonucleotides 5′-CCGCGAGCTCC GTACTGTTACTCTC-3′ (oRP171) and 5′-TTAAGCGATAAC ACAG-3′ (oRP59). This fragment was then digested with *Sac*I-*Bam*HI and ligated into *Sac*I-*Bam*HI pRP592 to yield pRP640. Plasmid RP641 was similarly constructed by PCR amplification of the PGK1-MFA2 fragment from pRP617 with the primers oRP171 and oRP59. This fragment was then digested with *Sac*I-*Bam*HI and ligated into *Sac*I-*Bam*HI pRP592 to yield pRP641. Plasmid RP638 was made by ligating the *Xba*I-*Hin*dIII fragment of pRP430 to *Xba*I-*Hin*dIII-digested pRP594. Plasmid RP639 was similarly constructed by ligating the *Xba*I-*Hin*dIII fragment of pRP430 to *Xba*I-*Hin*dIII-digested pRP618. The plasmid RP711 was created by PCR mutagenesis, where pRP594 was amplified with the oligonucleotides 5′-GGCC CAGATCTACCAACCTTAATGTCTTTATCTTCAAAGTTG-3′ (oRP233) and 5′-TTAGCGTAAAGGATGGGG-3′ (oRP25). This fragment was then digested with *Bgl*II and ligated to *Bgl*II-digested pRP594 to yield pRP711. Plasmid RP712 was made using PCR mutagenesis by first amplifying pRP469 with the primers 5′-GCAGCACCAGATCTACCAACCTTAA TGAGCCTTAGCAGTAAATTGTCTGTCCAAGATTTGG-3′ (oRP259) and oRP25. The PCR fragment was then digested with *Bgl*II and ligated into *Bgl*II-digested pRP549, to yield pRP712. In a similar fashion, pRP713 was constructed by first PCR amplifying PCR pRP469 with the oligonucleotide 5′-GCAGCACCAGATCTACCAACCTTAATGCAACCGATCAC CACTTTGTCTGTCCAAGATTTGG-3′ (oRP258) and oRP25. The PCR fragment was next digested with *Bgl*II and ligated to *Bgl*II-digested pRP549 to yield pRP713.

The mRNAs for the β-galactosidase expression assays were expressed from the following plasmids: PGK1-lacZ, pRP181; M-aug-P6P-lacZ, pRP908; PGK1Δ81-lacZ, pRP166; M-aug-P6PΔ81-lacZ, pRP909. In all these constructs the lacZ coding region was inserted in frame at the *Bgl*II site in the 3′ end of the PGK1 coding region. Liquid β-galactosidase assays were performed essentially as previously described (Beelman & Parker, 1994). Relative translation rates were determined by assigning the PGK1-lacZ fusion a value of 100% and then calculating the relative rates derived from the other fusion transcripts as standardized for mRNA concentration.

mRNA analysis

Steady-state mRNA experiments were performed as described (Caponigro et al., 1993). Yeast cultures were grown to mid-log phase in galactose medium at 24 °C, harvested, and shifted to dextrose medium at 36 °C to concomitantly inhibit transcription promoted by the *GAL*1 UAS and transcription by the temperature-sensitive *rpb1-1* allele of RNA polymerase II. Aliquots were then removed at each time point.

Transcriptional pulse-chase experiments were performed as described (Decker & Parker, 1993). Yeast cultures were grown to mid-log phase in raffinose medium at 24 °C, harvested, suspended in galactose medium at 24 °C for 8 min to induce transcription from the *GAL*1 UAS, and then shifted to 36 °C in dextrose medium to shut off transcription.

mRNA was isolated by glass-bead lysis of cells, followed by phenol, phenol-chloroform, and chloroform extractions, as previously described (Caponigro et al., 1993). Northern assays were performed on 10 μg of total RNA to determine RNA levels, as previously described. The Northern blots were quantitated with a Molecular Dynamics phosphorimager and standardized to the stable scRI RNA, an RNA polymerase III transcript (Felici et al., 1989).

Polyribosome analysis

Polyribosomes were prepared without cycloheximide and fractionated essentially as described by Atkin et al. (1995) with minor modifications. Two hundred microliters of yeast cultures were grown to mid-log phase in selective media with galactose as a carbon source at 24 °C and harvested by centrifugation. Cells were washed with lysis buffer (10 mM Tris-HCl, pH 7.5 at 4 °C, 0.1 M NaCl, 30 mM MgCl$_2$, 200 mg/mL heparin, and 0.2% DEPC), resuspended in 0.2 mL lysis buffer and lysed with glass beads at 4 °C. The lysed cells were spun at approximately 6,500 × *g* in a microcentrifuge at 4 °C and the supernatant was collected as the cellular polysome extract. Twelve microliters of 15–50% sucrose gradients were prepared in centrifuge tubes by layering 2.4 mL of sucrose solutions containing 50, 41.25, 32.5, 23.75, and 15% sucrose (from bottom to top) in gradient buffer (50 mM Tris-acetate, pH 7.0 at 4 °C, 50 mM NH$_4$Cl, 12 mM MgCl$_2$, 1 mM DTT, and 0.1% DEPC). Aliquots of 7.5 A260 U of cell extract were loaded onto the sucrose gradients and centrifuged at 39,000 rpm for 2.5 h in a SW41 rotor (Beckman Instruments). The OD254 profile of the gradient was determined with a continuous flow UV detector and chart recorder as the gradient was collected in 0.6 mL fractions. mRNA was isolated from each fraction by standard methods and analyzed on Northern gels.

ACKNOWLEDGMENTS

REFERENCES

Atkin AL, Altamura N, Leeds P, Culbertson MR. 1995. The majority of the yeast UPF1 co-localizes with polyribosomes in the cytoplasm. *Mol Biol Cell 6*:611–625.

Baim SB, Sherman F. 1988. mRNA structures influencing translation in the yeast *Saccharomyces cerevisiae*. *Mol Cell Biol 5*:1839–1846.

Beelman CA, Parker R. 1994. Differential effects of translation inhibition *in cis* and *in trans* on the decay of the unstable yeast MFA2 mRNA. *J Biol Chem 269*:9687–9692.

Beelman CA, Parker R. 1995. Degradation of mRNA in eukaryotes. *Cell 81*:179–183.

Beelman CA, Stevens A, Caponigro G, LaGrandeur TE, Hatfield L, Fortner DM, Parker R. 1996. An essential component of the decapping enzyme required for normal rates of mRNA turnover. *Nature 382*:642–646.

Brown BD, Zipkin ID, Harland RM. 1993. Sequence-specific endonucleolytic cleavage and protection of mRNA in *Xenopus* and *Drosophila*. *Genes & Dev 7*:1620–1631.

Caponigro G, Muhlrad D, Parker R. 1993. A small segment of the MATα1 transcript promotes mRNA decay in *Saccharomyces cerevisiae*: A stimulatory role for rare codons. *Mol Cell Biol 13*:5141–5148.

Caponigro G, Parker R. 1996. Mechanisms and control of mRNA turnover in *Saccharomyces cerevisiae*. *Microbiol Rev 60*:233–249.

Cereghino GP, Scheffler IE. 1995. Glucose-dependent turnover of the mRNAs encoding succinate dehydrogenase peptides in *Saccharomyces cerevisiae*: Sequence elements in the 5′ untranslated region of the Ip mRNA play a dominant role. *Mol Biol Cell 6*:1125–1143.

Cigan AM, Pabich EK, Donahue TF. 1988. Mutational analysis of the *HIS4* translational initiator region in *Saccharomyces cerevisiae*. *Mol Cell Biol 8*:2964–2975.

Decker CJ, Parker R. 1993. A turnover pathway for both stable and unstable mRNAs in yeast: Evidence for a requirement for deadenylation. *Genes & Dev 7*:1632–1643.

Felici F, Cesareni G, Hughes JMX. 1989. The most abundant small cytoplasmic RNA of *Saccharomyces cerevisiae* has an important function required for normal cell growth. *Mol Cell Biol 9*:3260–3268.

Gay DA, Sisodia SS, Cleveland DW. 1989. Autoregulatory control of β-tubulin mRNA stability is linked to translation elongation. *Proc Natl Acad Sci USA 86*:5763–5767.

Gera JF, Baker EJ. 1998. Deadenylation-dependent and -independent decay pathways for alpha1-tubulin mRNA in *Chlamydomonas reinhardtii*. *Mol Cell Biol 18*:1498–1505.

Gonzalez CI, Martin CE. 1996. Fatty acid-responsive control of mRNA stability. Unsaturated fatty acid-induced degradation of the *Saccharomyces* OLE1 transcript. *J Biol Chem 271*:25801–25809.

Heaton B, Decker C, Muhlrad D, Donahue J, Jacobson A, Parker R. 1992. Analysis of chimeric mRNAs derived from the STE3 mRNA identifies multiple regions within yeast mRNAs that modulate mRNA decay. *Nucleic Acids Res 20*:5365–5373.

Herrick D, Parker R, Jacobson A. 1990. Identification and comparison of stable and unstable mRNAs in *Saccharomyces cerevisiae*. *Mol Cell Biol 10*:2269–2284.

Hsu CL, Stevens A. 1993. Yeast cells lacking 5′ to 3′ exoribonuclease 1 contain mRNA species that are Poly(A) deficient and partially lack the 5′ cap structure. *Mol Cell Biol 13*:4826–4835.

Jacobs Anderson JS, Parker R. 1998. The 3′ to 5′ degradation of yeast mRNAs is a general mechanism for mRNA turnover that requires the SKI2 DEVH box protein and 3′ to 5′ exonucleases of the exosome complex. *EMBO J 17*:1497–1506.

Jacobson A, Peltz SW. 1996. Interrelationships of the pathways of mRNA decay and translation in eukaryotic cells. *Ann Rev Biochem 65*:693–739.

Kruys V, Huez G. 1994. Translational control of cytokine expression by 3′ UA-rich sequences. *Biochimie 76*:862–866.

Merrick WC, Hershey JWB. 1996. The pathway and mechanism of eukaryotic protein synthesis. In: Hershey JWB, Mathews MB, Sonenburg N, eds. *Translational control*. Cold Spring Harbor, New York: Cold Spring Harbor Laboratory Press. pp 31–70.

Muhlrad D, Decker CJ, Parker R. 1994. Deadenylation of the unstable mRNA encoded by the yeast MFA2 gene leads to decapping followed by 5′ → 3′ digestion of the transcript. *Genes & Dev 8*:855–866.

Muhlrad D, Decker CJ, Parker R. 1995. Turnover mechanisms of the stable yeast PGK1 mRNA. *Mol Cell Biol 15*:2145–2156.

Muhlrad D, Parker R. 1992. Mutations affecting stability and deadenylation of the yeast MFA2 transcript. *Genes & Dev 6*:2100–1211.

Muhlrad D, Parker R. 1994. Premature translational termination triggers mRNA decapping. *Nature 370*:578–581.

Nielsen FC, Christiansen J. 1992. Endonucleolysis in the turnover of insulin-like growth factor II mRNA. *J Biol Chem 267*:19404–19411.

Peltz SW, Donahue JL, Jacobson A. 1992. A mutation in the tRNA nucleotidyltransferase gene promotes stabilization of mRNAs in *Saccharomyces cerevisiae*. *Mol Cell Biol 12*:5778–5784.

Pierrat B, Lacroute F, Losson R. 1993. The 5′ untranslated region of the PPR1 regulatory gene dictates rapid mRNA decay in yeast. *Gene 131*:43–51.

Presutti C, Villa T, Hall D, Pertica C, Bozzoni I. 1995. Identification of the *cis*-elements mediating the autogenous control of ribosomal protein L2 mRNA stability in yeast. *EMBO J 14*:4022–4030.

Ross J. 1995. mRNA stability in mammalian cells. *Microbiol Rev 59*:423–450.

Yun D-F, Laz TM, Clements JM, Sherman F. 1996. mRNA sequences influencing translation and the selection of AUG initiator codons in the yeast *Saccharomyces cerevisiae*. *Mol Microbiol 19*:1225–1239.